Pediatric, Adult and Elderly Bone Material Properties

Damien Subit, Carlos Arregui, Robert Salzar, Jeff Crandall

Abstract As finite element models can be tailored to specific individual anthropometry, sex and age, there is a need for refined material properties. This study contributes to this effort by generating new data for the age-dependence in bone material properties in males. The left tibiae and femora were extracted from five male subjects aged 15 (pediatric subject), 37 and 40 (adult group), and 72 and 75 (elderly group). Small bone coupons were machined and tested under tensile load. The pediatric coupons (n = 15) were tested under quasi-static loading (~ 0.5 %/s). For the adult and elderly subjects (n = 16), two coupons were harvested next to each other to create matched pairs: one was tested under quasi-static loading and the other one was tested under dynamic loading (~ 100%/s). An optical stereophotogrametric non-contact system was used to measure the strain field on the outermost surface of each coupon. The adult and elderly coupons were found to be elastic, with brittle fracture, and were on average 15 % more compliant in quasi-static than in dynamic. The pediatric coupons exhibited an elasto-plastic behaviour, and were on average 15 % more compliant that the adult coupons.

Keywords age dependence, bone, coupon, full field strain measurements, quasi-static and dynamic tensile tests

I. INTRODUCTION

Finite element models are developed to assist safety researchers and engineers to design new safety systems and evaluate their performance. Accessing the geometry of the human body is not a technical challenge anymore with the increased use of non-invasive and non-destructive medical imaging tools such as computed tomography and resonance imaging technologies [1,2]. This allows researchers to build geometrical models of the human body for various age and sex with the view to using them as a basis for the development of computational human body models. Element sizes have drastically dropped to allow for a very detailed reconstruction of the geometry of bony structures to include the cortical and trabecular bones. These refined finite element models can now capture small geometrical features such as the variation in the thickness of the cortical layer, and can be used to predict fracture. However, the bone material properties currently available, and in particular the age and rate sensitivity, have been mainly determined from compression tests [3] or based on tests where the strain in the bone was derived from the applied displacement rather than directly measured [4], or measured with a physical extensometer, a tool that is known to have slippage problems for high strain rate [5]. Therefore, the goal of the present study was to implement the use of an optical technique (digital image correlation) to measure strain in bone coupons with a non-contact system, by carrying out a series of quasi-static and dynamic tests on bone coupons harvested from the lower extremities of pediatric, adult and elderly human subjects.

II. MATERIALS AND METHODS

Small bone samples were extracted from the shaft of the tibiae and femora of five post mortem human subjects (PMHS). Each sample was then tested under either quasi-static or dynamic loadings, and the surface deformation was measured with a non-contact optical system.

Subjects information

Five male PMHS were selected for this study (Table 1) based on the absence of pre-existing fractures, lesions or other bone pathology, as confirmed by pre-test computed tomography (CT) analysis. The cadavers were obtained and treated in accordance with the ethical guidelines established by the National Highway Traffic Safety Administration, and all testing and handling procedures were reviewed and approved by an independent oversight committee at the University of Virginia. Upon arrival, the PMHS were refrigerated (2˚C) for 8 to 32

D. Subit is a Senior Scientist at the University of Virginia - Center for Applied Biomechanics (UVA-CAB), Charlottesville, VA, USA (Ph: +1 434 296 7288 x 148, Fax: +1 434 296 3453, subit@virginia.edu), C. Aarregui is a Professor Lector (lecturer) at the Universitat Politecnica de Catalunya, Spain, R. Salzar is a Principal Scientist at UVa-CAB, J. Crandall is Professor at UVa and director of UVa-CAB.

hours pending blood test results for infectious diseases. Provided the blood screening was negative, the subjects were stored in a freezer (-15˚C) until they were removed and placed at room temperature for about 24 hours, until the lower extremities were thawed.

Table 1. Subjects information.

Group	Subject id	Age (year)	Height (cm)	Weight (kg)	Cause of death
Pediatric	485	15	163	50	Brain Tumor (Malignant Thalamic Glioblastoma)
Adult 1	441	37	188	92.6	Seizure Disorder, Chronic Alcoholism
Adult 2	482	40	185	83	Brain Cancer
Elderly 1	481	72	173	87.5	Cardiopulmonary Arrest
Elderly 2	476	75	173	78.5	Cardiovascular disease

Samples information

Samples harvest location

The coupons were harvested from the mid shaft of the left tibiae and femora. For the adult and elderly subjects, two coupons (indexed A and B) were prepared: the two coupons were sliced next to each other, with A being the outermost sample. For the pediatric subject, coupons in the femur were taken from the medial aspect of the femur (samples A to D) and from the lateral aspect of the femur (samples A to E), with A being the outermost sample, and D or E being the innermost ones (the closest to the medullar canal). For the pediatric tibia, samples were harvested from the lateral (samples A and B), medial (samples A and B) and posterior aspects (samples A to C) of the bone.

Coupon shape

Bone coupon shape and dimensions were chosen based on Kemper et al [4] and Subit et al [6] (Figure 1). The coupons were made as thin as possible to be able to consider that two coupons sliced next to each other have the same bone characteristics and allow for the comparison of the quasi-static and dynamic test results. In addition, by matching the dimensions used by Subit et al [6] for the rib cortical bone, it will be possible to compare the bone properties measured for the rib and lower extremity bones in the future.

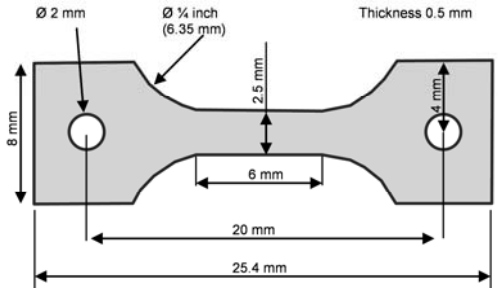

Figure 1. Dimensions of the bone coupon. The two holes are used only for references for machining and testing, and do not carry any load.

The method for the preparation of the samples and the test apparatus were designed by Subit et al [6], and they are outlined in the next two sections.

Sample preparation

Thick longitudinal slices of the tibia and the femur were harvested at the mid shaft level for each subject. The coupons were machined in the longitudinal direction of the bones. First, a slab of cortical bone was cut in the cortical shell using an abrasive band saw equipped with a diamond blade (Diamond bone band saw, Mar-med Inc., Cleveland, OH, USA) (Figure 2, a and b). The band saw allows for making cuts that approximately shape the bone slab to the appropriate dimension. The next cuts were performed with a low speed diamond saw (IsoMet low speed saw, Buehler Ltd, Lake Bluff, IL, USA, equipped with a 15HC Diamond blade) that can execute parallel cuts with micrometric accuracy (Figure 2, c and d). The sample was glued to a piece of hard foam that was then clamped in the sample holder in the desired orientation thanks to screws with spear tips.

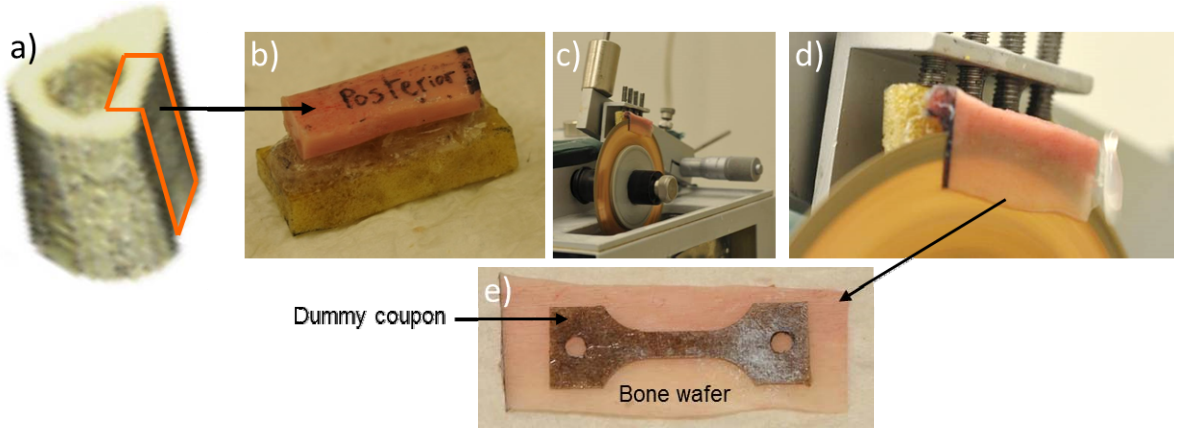

Figure 2. Machining of bone wafers from the shaft cut-out to the bone wafer.

The next step consisted in machining the bone wafer to give it the final shape. This happened in two successive actions. First, the wafer was machined down to the right length and, second, the narrow section of the coupon was made. These two actions utilized the same principle. After the two holes were drilled in the wafer (as shown in Figure 1), the wafer was sandwiched between two pieces of Delcron ™ and attached thanks to two screws to a template made of brass (Figure 3). A router equipped with a bearing router bit was used to trim down the bone wafer to the desired shape: the bearing at the top of the router bit (Figure 3, a) was kept in contact with the brass template that was used as a guide. Two templates were used: one to shorten the wafer to the desired length (Figure 3, b), and one to machine the coupon to the desired shape (Figure 3, c and d). For the shape, the template was designed with two grooves (Figure 3, c): after the first side was machined, the wafer was rotated about one screw and set along the other groove to trim down the non-machined side. The final thickness and width of the gage area were measured for all the coupons to determine the cross-sectional area. Finally, the coupons were stored in a tube filled with 0.9 % saline solution and kept in a fridge until the test day (3 to 4 days after preparation) to ensure proper conservation.

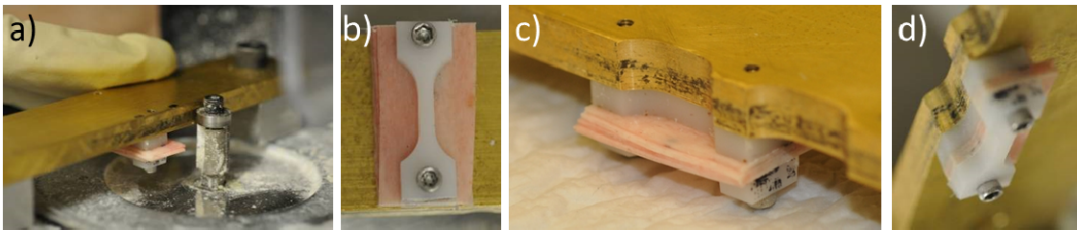

Figure 3. Machining of the bone wafer to create the final coupon.

Experimental set-up

The tests were run on a standard tensile machine (Model 8874, Instron Inc, Norwood, MA, USA), to which a custom designed test fixture was affixed. Displacement was applied at 0.01 mm/s for the quasi-static tests (estimated strain rate: 0.07 %/s) and 15 mm/s for the dynamic tests (estimated strain rate: 100 %/s). The loading rates were estimated from knee impact tests reported on in Salzar et al [7] where the strain rate in the tibia was between 20 and 175 %/s.

A clamping system was designed to avoid misalignment between the top and the bottom ends of the coupon. Because of the fragility of the coupon, it was critical to be able to install it for testing without applying any loads that could generate bending, shear or too much tension. Conventional fixed wedge clamps would not ensure the required control of the load during the installation of the coupon. As the breaking force was expected to be less than 300 N, small low-mass clamps were designed to be attached to the coupon (Figure 4). Each clamp weighed 10.9 grams.

The two rod-end ball joints provided three rotational degrees of freedom. The clamps were orientated 90 degrees with respect to each other. Rigid pins were used to affix the coupon equipped with the clamps to the machine (Figure 5). Pins could slide and rotate at both ends to ensure that no shear/bending/torsion loads were applied to the sample before test. The top pin was first installed. The bottom pin was initially installed without

touching the bottom clevace. The sample was then put in a vertical position by adjusting the position of the pins and carefully put under tension by moving up the top clevace (connected to the Instron piston). Once the sample was put under tension, the pins could not move any more. About 2 N in quasi-static and 6 to 7 N in dynamic were applied to avoid any inertial loading due to the acceleration of the lower clamp when the displacement was applied. A three-axis load cell connected the bottom clevace to the base of the Instron machine, and the top clevace was connected to the piston.

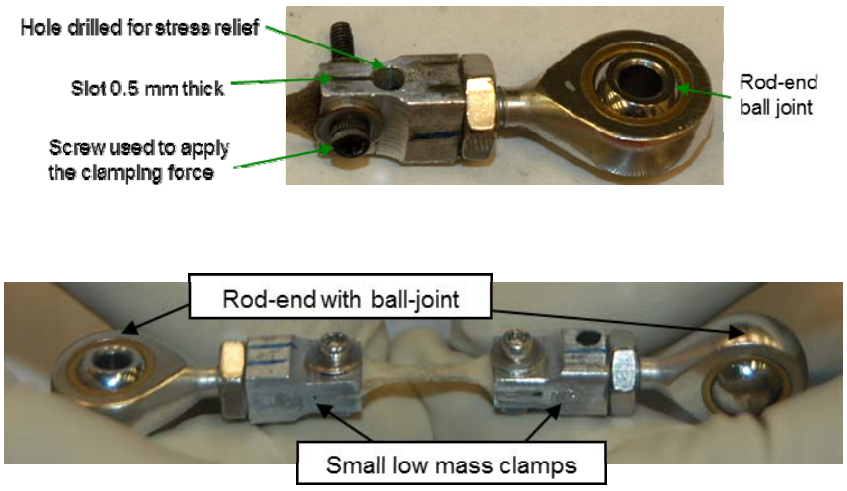

Figure 4. Clamps designed to hold the coupon to prevent misalignment.

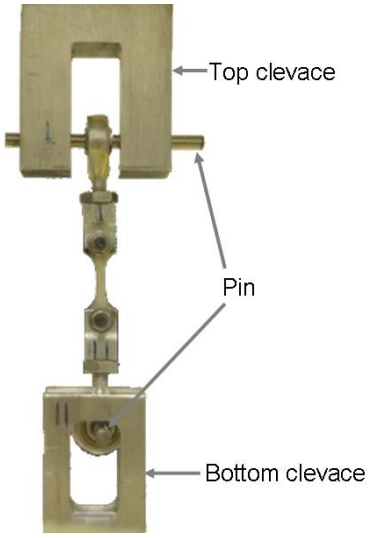

Figure 5. Clamping device.

Data collection

A standard data acquisition system (DEWE-2010, Dewetron GmbH, Graz, Austria) was used for the measurement of the load cell and the displacement output. The sampling rate was 5,000 Hz for the quasi-static tests and 100,000 Hz for the dynamic tests. The strain was measured by tracking the deformation of a speckle pattern created on the sample with spray paint (Figure 6). Images were recorded with a Redlake HG-100K high speed camera equipped with a macro lens (Nikon AF 105mm) at a rate of 30 fps (frames per second) for the quasi-static tests and 6115 fps for the dynamic tests. Only one camera was necessary since the coupons were machined flat and the load was applied in the plan of the coupon. A fiber optic lighting system (Dolan-Jenner MI-150 Fiber Optic Illuminator, Edmunds Optics, New Jersey, USA) was used to provide the amount of light required in particular for high speed videos: fiber lights provide a continuous light (they are powered by continuous current and therefore do not flicker) and reduce the heat output compared to incandescent lights. The positioning of these lights was finely adjusted to output the best contrast.

Figure 6. Black and white speckle pattern applied to the coupon outer surface.

The Aramis software package (V6.2, GOM, GmbH) was used to determine the strain field on the outer surface of the coupons. The software tracks the deformation of the speckle pattern by image correlation, and this deformation is used to determine the strain field.

Bone material properties

The stress was calculated as the tensile force divided by the initial cross-section in the middle of the gage area. The force signals were smoothed using a moving average over five points to remove any noise. A virtual extensometer was defined in the Aramis software to estimate the tensile strain in the coupon (Figure 7). The bone was assumed to be homogeneous isotropic. The yield strain and stress were determined as the point

where the stress-strain curve inflexes, and these values were used to determine the Young's modulus. Failure strain and failure stress were determined as the last positive values before the stress goes back to zero (or to a negative value) because of the fracture.

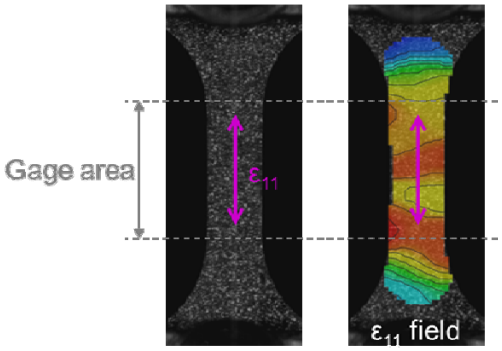

Figure 7. Definition of the tensile strain based on digital image correlation.

Text matrix

All the pediatric coupons were tested under quasi-static loading. For the adult and elderly coupons, the coupons indexed 'A' were tested under quasi-static loading (0.01 mm/s), while the coupons indexed 'B' were tested under dynamic loading (15 mm/s).

III. RESULTS

Stress-strain curves

The stress-strain curves were plotted for the pediatric coupons (Figure 8), the adult coupons (Figure 9) and the elderly coupons (Figure 10). In the pediatric series, the coupon Tibia posterior A broke during handling and could not be tested. For the adult subject 2, the femur coupon tested under quasi-static loading exhibited a peculiar behavior believed to be due to slippage in the clamp area. Therefore the results for these tests were not included.

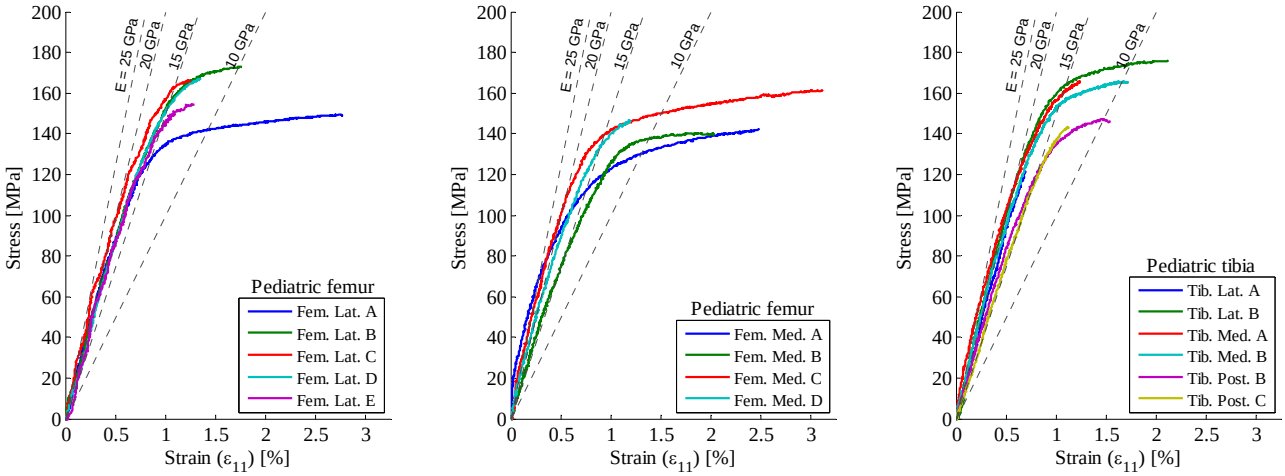

Figure 8. Stress-strain curves for the pediatric coupons (left: lateral femur, center: medial femur, right: tibia).

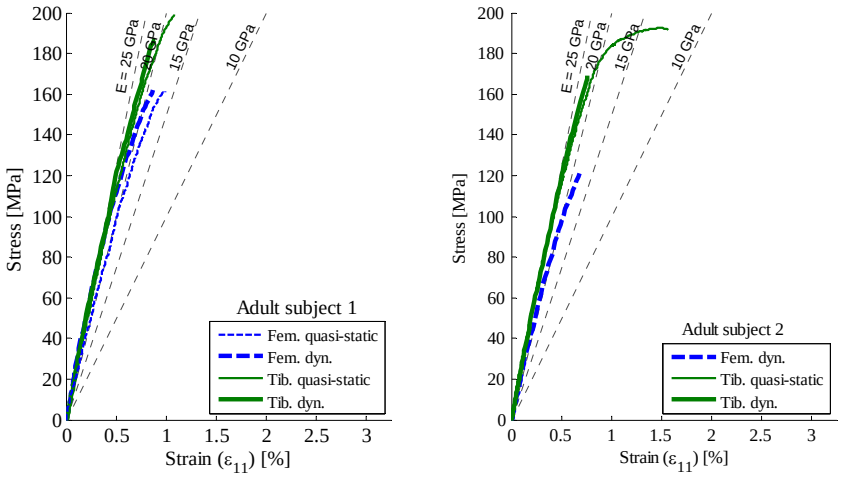

Figure 9. Stress-strain curves for the adult coupons. Fem.: femur, Tib.: tibia, dyn.: dynamic.

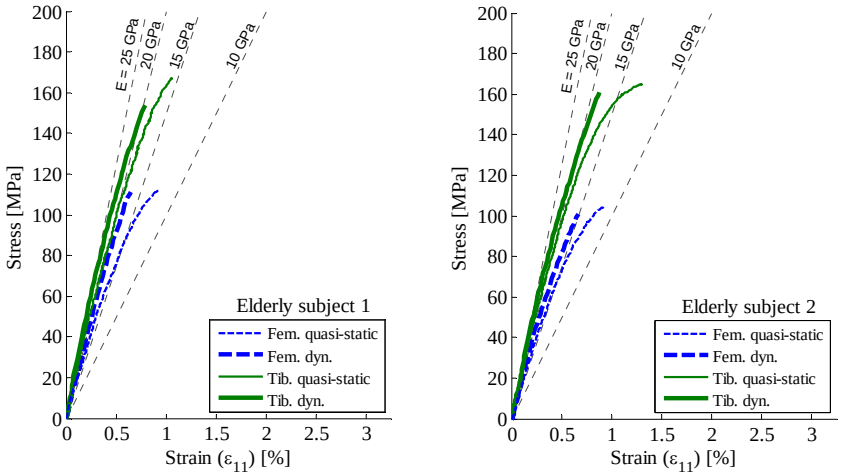

Figure 10. Stress-strain curves for the elderly coupons. Fem.: femur, Tib.: tibia, dyn.: dynamic.

Bone material properties

The material properties estimated from the stress-strain curves are summarized in Table 2 and Table 3.

Table 2. Material properties for the pediatric subject.

Coupons	E [GPa]	Yield strain [%]	Failure strain [%]	Yield stress [MPa]	Failure stress [MPa]	Strain rate [%/s]
Femur lateral A	15.5	0.8	2.76	124.3	149.4	0.081
Femur lateral B	15	1.02	1.75	154.4	172.5	0.056
Femur lateral C	17.3	0.84	1.24	145.6	165.6	0.057
Femur lateral D	16	0.87	1.35	138.2	166.4	0.059
Femur lateral E	16.1	0.88	1.29	135.7	154.4	0.057
Femur medial A	14	0.82	2.47	115.7	141.7	0.087
Femur medial B	12.1	1.08	2.03	131	139.8	0.078
Femur medial C	17.4	0.76	3.11	130.6	160.8	0.088
Femur medial D	14.6	0.93	1.19	136	145.9	0.062
Tibia lateral A	17.7	N/A	0.69	N/A	120.9	0.04
Tibia lateral B	17.3	0.91	2.11	178.2	175.9	0.068
Tibia medial A	16.1	0.95	1.23	154.1	164.7	0.044
Tibia medial B	15.4	0.99	1.72	152.7	165	0.041
Tibia posterior B	14.1	0.93	1.53	130.6	145.6	0.065
Tibia posterior C	14.6	0.85	1.12	123.7	143	0.06

Table 3. Material properties for the adult and elderly subjects. Dynamic tests are in bold characters.

Subject	Bone	E [GPa]	Yield strain [%]	Failure strain [%]	Yield stress [MPa]	Failure stress [MPa]	Strain rate [%/s]
Adult 1	Femur	17.9		0.99		160.9	0.049
		21.9		**0.86**		**157.4**	**87.1**
	Tibia	19.2		1.08		178.4	0.049
		23.7		**0.88**		**185.1**	**78.3**
Adult 2	Femur	N/A					
		20.8		**0.67**		**122.6**	**97.9**
	Tibia	21.9		1.57		197.4	0.045
		21.8		**0.75**		**162.3**	**77.6**
Elderly 1	Femur	16.3	0.67	0.92	109.6	126.1	0.055
		19.7		**0.64**		**117.7**	**96.9**
	Tibia	18.4		1.05		157	0.035
		23.2		**0.78**		**153.9**	**84.5**
Elderly 2	Femur	14.6		0.92		100.9	0.052
		16.7		**0.66**		**97**	**100.3**
	Tibia	19.9		1.3		180.5	0.05
		22.1		**0.88**		**168.2**	**82.7**

IV. DISCUSSION

Validity of the experimental set-up

The characterization of the bone material behavior presents three main challenges: (1) the preparation of the samples, (2) the installation of the sample and (3) the measure of the strain. The method presented in this study was found to be effective to prepare coupons of constant size. By choosing to machine thin coupons (nominal thickness of 0.5 mm), the design can be used for other bone such as the rib cortical bone [6] and the skull bone [8]. Only two samples could not be used in this study: one broke during handling and one broke in the clamp. For the second one, the issue was most likely an uneven surface in the clamp, or the clamping force was too small. The screws that compress the clamp (Figure 4) have to bear a large load, and they need to be replaced almost every other test because their thread gets damaged easily. Regarding (3), the use of a non-contact optical system instead of strain gauges to measure the strain had at least two advantages. First, strain gauges have to be glued to the surface of the bone, which may lead to the stiffening and embrittlement of the samples because of the glue penetrating the bone pores, and the stiffness of the strain gauge itself. Second, it provides full field strain which allows to control that the samples were loaded in tension. In Figure 11 that shows a snapshot of the displacement on the outer surface of a coupon immediately prior to fracture, the displacement in the tensile direction (direction 1) is virtually independent on the position in direction 2, and the displacements in direction 2 are very small (less than 0.0081 mm in absolute value). The displacement field confirmed that the coupons were loaded in tension.

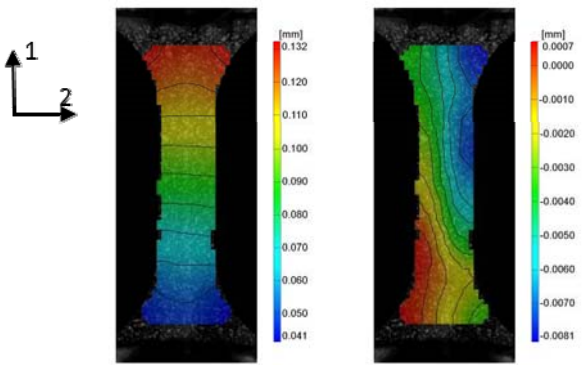

Figure 11. Displacement in the coupon gage area, in the tensile (vertical) direction on the left, and in the direction orthogonal to the tensile direction (horizontal) on the right (coupon: adult 2, tibia, dynamic).

Rate sensitivity for the adult and elderly coupons

The Young's moduli measured for the adult and elderly subjects are in line with the data available in the

literature [4-5, 9]. However, the behavior of the bone was found to be elastic, with nearly no plasticity. The sensitivity to the loading rate could be evaluated by assuming that two coupons harvested next to each other have similar mechanical properties. Young's moduli were found to be greater in dynamic than in quasi-static, whereas the failure stress was found to be nearly insensitive (ratio close to 1, Figure 12). As a consequence, the failure strain was smaller in dynamic than in quasi-static.

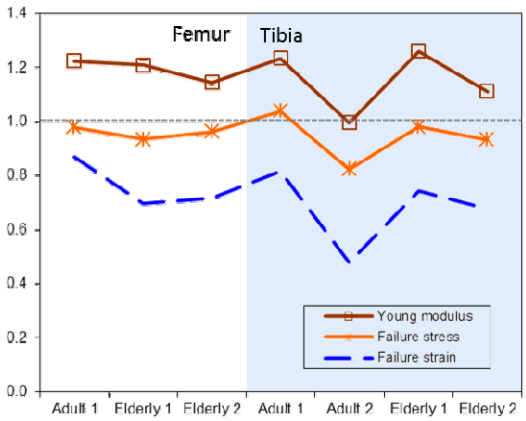

Figure 12. Ratios of the Young's moduli, failure stresses and failure strains (dynamic values divided by the quasi-static values) for the adult and elderly subjects.

Age dependence

The pediatric coupons were found to have a non linear behavior, that is most likely plasticity (the coupons were not unloaded prior to fracture, therefore there are no data to confirm this). In addition, the material properties were found to be age-dependent (Figure 13), with a lower Young's modulus for the pediatric subject compared to the adult and elderly one. The failure stress increases between the pediatric and adult subjects, and decreases with increasing age. As for the failure strain, the results are spread for the pediatric subject, which is consistent with the plastic behavior and the large variability observed between coupons. The data reported on in McCalden et al [10] were somewhat different, with no age dependence observed for the Young's modulus, and decreasing trends observed for both the failure strain and failure stress when age increases. While McCalden et al tested 235 specimens, only 31 were tested in the current study, and the differences in the results may have an effect of the sample sizes. However, the specimens used by McCalden et al were larger than those tested in the current study and they had a square 2×2 mm cross-section. This difference in design may have an effect on the measured bone properties, as the stress distribution was different in these two designs which could lead to different yield/failure mechanisms.

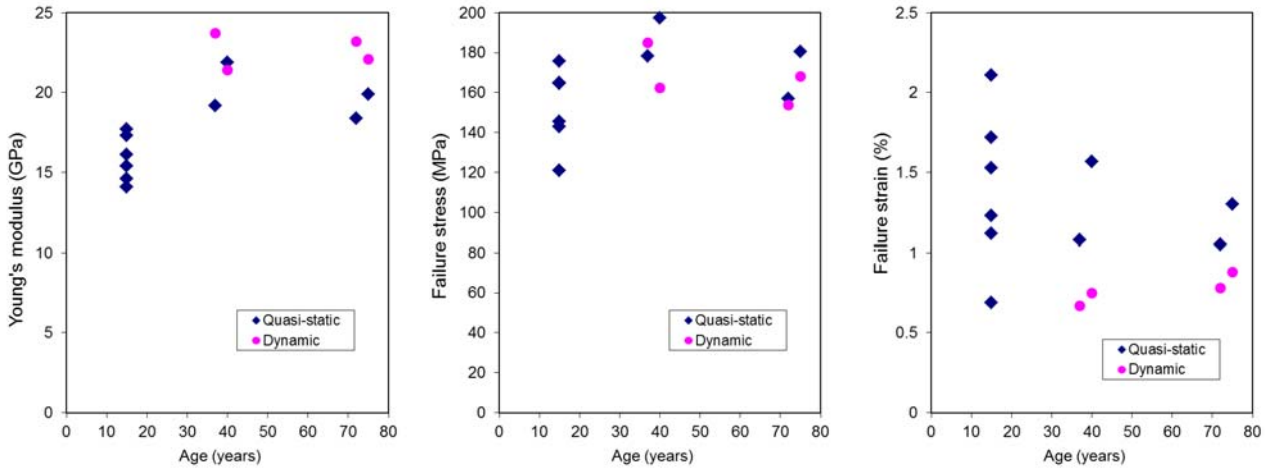

Figure 13. Variation of the bone material properties as a function of age (for the tibia coupons only).

Comparison of the bone material properties for the tibia and femur

The tibial specimens had on average 25.6 % greater Young's modulus and 13.8 % greater failure stress than the femoral specimens. This result was also reported in Burstein et al [11] and McCalden et al [10]. It was

hypothesized that these differences are caused by different bone remodeling rates in these two bones, which is the result of different loading conditions. Unfortunately, none of the results presented in the current study can be used to evaluate this assumption.

Bone condition for the pediatric subject

The pediatric subject had a brain tumor and had most likely received chemotherapy. There is ongoing research to determine how bone cells react to chemotherapy, as it is suspected to cause osteoporis and osteomalacia. Osteomalacia is the softening of the bones due to a lack of vitamin D or a problem with the body's ability to break down and use this vitamin: for a person with osteomalacia, bones have a normal amount of collagen, but lack the proper amount of calcium. The pediatric specimens tested in the present study had indeed lower Young's moduli than the adult and elderly specimens. They also exhibited greater plasticity. While no data allows to confirm whether the pediatric subject had osteomalacia, the failure strains calculated in this study are consistent with those reported in Hirsch and Evans [12] and Lindhal and Lindgren [13].

V. CONCLUSIONS

This paper presented a methodology to prepare and test bone coupons under quasi-static and dynamic tensile loadings. The results of thirty-one coupon tests were presented and analyzed to estimate the femur and tibia bone material properties. The coupons extracted from the pediatric subject exhibited an elasto-plastic behavior, with a lower Young's modulus compared to the adult (37 and 40 year old) and elderly (72 and 75 year old) groups. The adult and elderly coupons were found to be elastic with brittle fracture most often, and their material properties were rate-dependent. The coupons extracted from the tibia had a greater Young's modulus than those extracted from the femur. Although this study includes a limited number of samples, and only one pediatric subject that had a medical condition that could affect the bone properties, the result presented here are consistent with the literature. Further analysis of the strain distribution within the bone samples will allow to estimate additional material parameters, such as the Poisson's ratio, and look into the relationship between the bone microstructure (presence of pores in the samples) and the location of fracture.

VI. ACKNOWLEDGEMENT

The authors would like to acknowledge the funding of Honda R&D Co. Ltd., Japan, for the adult and elderly coupon tests.

VII. REFERENCES

[1] Vezin P and Verriest JP, Development of a set of numerical human models for safety, *Conference on Enhanced Safety Vehicles*, 2005.

[2] Gayzik FS, Moreno, DP, Danelson KA, McNally C, Klinich KD, Stitzel JD, External landmark, body surface and volume data of a mid-sized male in seated and standing postures, *Ann Biomed Eng,* 40(9): 2019-2032, 2012.

[3] McElhaney J, Dynamic response of bone and muscle tissue, *J Appl Physiol,* 21(4):1231-6, 1966.

[4] Kemper A, McNally C, Pullins C, Freeman L, Duma S, Rouhana S, The biomechanics of human ribs: material and structural properties from dynamic tension and bending tests, *Stapp Car Crash Journal,* 5:235-73, 2007.

[5] Hansen U, Zioupos P, Simpson R, Currey JD, Hynd D, The effect of strain rate on the mechanical properties of human cortical bone, *J Biomech Eng,* 130(1), 2008.

[6] Subit D, del Pozo E, Velázquez-Ameijide J, Arregui-Dalmases C, Crandall J, Tensile material properties of human rib cortical bone under quasi-static and dynamic failure loading and influence of the bone microstructure on failure characteristics, http://arxiv.org/abs/arXiv:1108.0390.

[7] Salzar RS, Lievers WB, Frimenko RE, Seamon J, Keller T, Subit DL, Gochenour TH, Sochor M, Crandall JR, Fracture tolerance of the patellofemoral joint in frontal knee impacts of 75 and 35 year old males, *International Journal of Crashworthiness,* 16(4):397-409, 2011.

[8] Boruah S, Subit D, Salzar R, Bone material properties of the adult human skull, *83rd Annual Meeting of Aerospace Medical Association,* 2012.

[9] Crowninshield R, Pope M, The response of compact bone in tension at various strain rates, *Annals of Biomedical Engineering,* 2(2):217-225, 1974.

[10] McCalden RW, McGeough JA, Barker MB, Court-Brown CM, Age-related changes in the tensile properties of cortical bone. The relative importance of changes in porosity, mineralization and microstructure, *J Bone Joint Surg - American volume,* 75(8):1193-1205, 1993.

[11] Burstein AH, Reilly DT, Martens M, Aging of bone tissue: mechanical properties, *J Bone Joint Surg - Amer volume,* 58(1):82-86, 1976.

[12] Hirsch C, Evans FG, Studies on some physical properties of infant compact bone, *Acta Orthop Scand,* 35:300-13, 1965.

[13] Lindahl O, Lindgren AGH, Cortical bone in man, II. Variation in tensile strength with age and sex, *Acta Orthop Scand,* 38(2):141-7, 1967.